Structural Engineering and Mechanics, *Vol. 66, No. 4 (2018) 505-513*
DOI: https://doi.org/10.12989/sem.2018.66.4.505

Geomechanical and thermal reservoir simulation during steam flooding

Roohollah Taghizadeh[1a], Kamran Goshtasbi[*2], Abbas Khaksar Manshad[3b] and Kaveh Ahangari[1c]

[1]*Department of Mining Engineering, Science and Research Branch, Islamic Azad University, Tehran, Iran*
[2]*Department of Mining Engineering, Faculty of Engineering, Tarbiat Modares University, Tehran, Iran*
[3]*Department of Petroleum Engineering, Faculty of Petroleum Engineering, Petroleum University of Technology, Abadan, Iran*

(Received May 14, 2017, Revised February 14, 2018, Accepted February 22, 2018)

Abstract. Steam flooding is widely used in heavy oil reservoir with coupling effects among the formation temperature change, fluid flow and solid deformation. The effective stress, porosity and permeability in this process can be affected by the multi-physical coupling of thermal, hydraulic and mechanical processes (THM), resulting in a complex interaction of geomechanical effects and multiphase flow in the porous media. Quantification of the state of deformation and stress in the reservoir is therefore essential for the correct prediction of reservoir efficiency and productivity. This paper presents a coupled fluid flow, thermal and geomechanical model employing a program (MATLAB interface code), which was developed to couple conventional reservoir (ECLIPSE) and geomechanical (ABAQUS) simulators for coupled THM processes in multiphase reservoir modeling. In each simulation cycle, time dependent reservoir pressure and temperature fields obtained from three dimensional compositional reservoir models were transferred into finite element reservoir geomechanical models in ABAQUS as multi-phase flow in deforming reservoirs cannot be performed within ABAQUS and new porosity and permeability are obtained using volumetric strains for the next analysis step. Finally, the proposed approach is illustrated on a complex coupled problem related to steam flooding in an oil reservoir. The reservoir coupled study showed that permeability and porosity increase during the injection scenario and increasing rate around injection wells exceed those of other similar comparable cases. Also, during injection, the uplift occurred very fast just above the injection wells resulting in plastic deformation.

Keywords: effective stress; multi-physical coupling; porous media; volumetric strain; permeability

1. Introduction

Thermal oil recovery is by far the most popular method used in the world during the tertiary stage of oil recovery. As an enhanced oil recovery (EOR) method and a major thermal stimulation of oil reservoirs, steam flooding has turned into an increasingly common method for extracting heavy crude oil helping the production of up to 30% of original oil in place. Steam injection does not pose as many environmental risks as other EOR methods may making it a viable technology in different countries even under strict regulations with economy as the main factor determining whether the technology should be implemented in one field or the other.

In a steam flood, sometimes known as a steam drive, some wells are used as steam injection wells and others are used for oil production. Many factors interact during this thermal process such as changes in oil viscosity, fluid saturations, pore pressure and stresses state.

The success of steam flooding has been demonstrated by both field and numerical simulation studies. The prediction of steam flooding performance by numerical simulation is an integral component in the design and management of a steam EOR project. In the conventional reservoir modelling approach, multiphase flow in porous media is computed but generally the geomechanical effects are not taken into account. Unfortunately, this assumption is not valid for reservoir rocks due to their high sensitivity to pore pressure and temperature variations.

Traditionally, more emphasis has been given to solve the flow problem alone by assuming a constant state of stress (total stress) in the system incorporating a time-invariant rock compressibility term for the complete mechanical response of the system. Conventional simulators neglect the interaction of a reservoir with its over-burden, under-burden and side-burden and implicitly assume equivalence of reservoir conditions under laboratory conditions during which the rock compressibility was measured leading to oversimplification of the physics governing fluid flow and geomechanics interactions (Longuemare *et al.* 2002).

Continuous steam injection triggers complex thermal and hydraulic processes which can dramatically alter the formation pressure and temperature leading to various changes within the reservoir as well as in the surrounding rocks. As steam is injected, the pressure and temperature in the reservoir rise. The increased temperature and pressure cause changes in field stresses, rock properties, porosity, and permeability, obviously a coupled problem necessitating coupled reservoir geomechanical simulations. A general review with respect to THM coupled processes is given in Wang *et al.* (2009), Watanabe *et al.* (2010) and Kolditz *et al.* (2012). To take into account the geomechanical effects due to stress changes in and around

*Corresponding author, Associate Professor
E-mail: goshtasb@modares.ac.ir
[a]Ph.D. Student
[b]Assistant Professor
[c]Asssociate Professor

http://www.techno-press.com/journals/sem&subpage=7 ISSN: 1225-4568 (Print), 1598-6217 (Online)

the reservoir, fluid flow must be solved in a way that can predict the evolution of stress dependent parameters such as porosity, pore compressibility and permeability (Goodarzi *et al.* 2010, Lynch *et al.* 2013, Lamy-Chappuis *et al.* 2015, Angus *et al.* 2015, Elyasi *et al*. 2016a, Elyasi *et al*. 2016b).

The work presented in this paper was performed in the framework of a study on reservoir-geomechanics thermo-hydro-mechanical (THM) coupling methods. Steam flooding coupled thermo-hydro-mechanical modeling is conducted using ECLIPSE 300 as the fluid flow (reservoir) simulator and ABAQUS as the geomechanical simulator. The objectives of this work are to emphasize the necessity of solving the coupled fluid flow and geomechanical effects that prevail during steam injection, to present the various possible options to cope with this difficult issue of coupling fluid flow and geomechanics, to evaluate the changes in stress state, porosity and permeability due to the changes in pore pressure and temperature. First, a description of the problem and the general methodology is presented providing an overview of workflow. Next, the application of this approach to a realistic test case has been illustrated. Finally, we conclude with a discussion of the results obtained.

2. Effect of increased pressure

In the porous rock, the normal stress (σ) at any point within the rock matrix is shared by the grains and the water held within the pores. The component of normal stress acting on the grains, is called effective stress and is generally denoted by σ. Geomechanical calculations consider effective stress in failure analysis which can be represented mathematically,

$$\sigma' = \sigma - \alpha P_p \tag{1}$$

Where σ' is the effective stress (net stress carried by the rock matrix), σ is total stress acting on the rock mass, P_p is pore pressure and α is Biot's poroelastic coefficient (approaching unity in highly porous media).

Effective stress depends on pore pressure. The higher the pore pressure, the lower the effective stresses. When steam is injected, in spite of temperature, pore pressure in the reservoir increases. This not only decreases effective stress but also exerts several other effects on the mechanical behavior of rock as described below.

- Injection pressure increases pore pressure which in turn decreases the confining pressure. At low confining pressures, the shear strength of rock reduces significantly (Handing and Hager 1957), making rock readily susceptible to failure in shear.

- Increases in pore pressure can cause (i) dilation within steam chamber as well as the adjacent layers, (ii) transient increase in overburden and horizontal stress within the steam chamber, and (iii) deficiency in horizontal stresses at the boundary of steam chamber among many other effects. These effects can lead to micro shear fractures in the cap layer right above the reservoir.

- Increases in the formation pressure decrease the effective stress making the exiting fractures or faults more susceptible to reactivation.

- If effective stress decreases significantly going below the tensile cut-off, inadvertent hydraulic fracturing can occur at the reservoir boundaries with the potential for such fractures to grow upwards into and through the caprock.

3. Effect of increased temperature

Increasing temperatures during steam injection can induce a significant amount of thermal strain

$$\sigma_T = \frac{\beta E \Delta T}{1 - \vartheta} \tag{2}$$

Where σ_T is the thermal stress, β is thermal expansion coefficient, T is temperature, E is Young's Modulus and ϑ represents Poisson ratio.

For instance,

- Although there will be an instantaneous increase in overburden stress due to high injection rate and rise in temperature, this increment can subside partly in the form of surface heave as there is no constraint on the free ground surface. However, due to lateral constraint from the adjacent rock, horizontal stresses experience large increases. This contrast creates shear fractures within the reservoir which is suitable for increasing reservoir permeability, but when these fractures extend to inter-bed boundaries, they can ultimately lead to generalized shear failure at cap rock interface.

- Mechanical properties of rock are temperature dependent. Stiffness and strength decrease with increasing temperature (Horsud 1998, Lempp and Welte 1994). Tensile strength as well as compressive strength can decrease remarkably in shale as temperature increases. In a study conducted by Closmanna and Bradley (1979), Young's modulus showed a considerable decrease with temperature.

- When temperature difference exceeds 80-100 C^0, yielding can be expected even in materials such as oil sands that are less stiff and unconsolidated than highly competent rock such as a carbonates. In softer rocks, stress changes are less than what is the case in stiff rocks, but the stresses needed for yielding are far lower because soft rocks like unconsolidated sandstone are much weaker than stiff rocks (Dusseault 2008).

4. Integrated geomechanics approach

In a reservoir, the mechanical deformations and fluid flow are coupled to each other. This coupling can be significant in reservoirs containing compressible rock. Coupled reservoir geomechanics analyses aim to identify the mechanical deformations due to oil and gas extraction, and to simultaneously include the changes in fluid flow resulting from mechanical deformations in the reservoir rock. Fluid flow modeling involves sophisticated analyses that need to include multiple fluids and fluid components differentiated according to the molecular weight of the constituent hydrocarbon fluids. The fluids can undergo dissolution and chemical changes depending on the prevailing pressures and temperatures. The pressure of the fluid leads to modifications in the stress regime in the rock which in turn can give rise to rock deformations and strains. An optimized operation during production and injection should be safe for reservoir and caprock integrity from the point of view of production. Optimized safe operating pressure depends on several key items including rock mechanical parameters, rock strength, in-situ stress condition and changes in reservoir petrophysical properties like porosity, permeability and stress variations due to injection. In order to estimate these parameters as accurately as possible, data from the following sources are essential:

- Seismic measurements and drill logs to describe the geometry of the layers in the ground. This information is spatial, i.e., in 3D. By itself, this information is difficult to use for simulation purposes. Therefore, the information is first examined by expert geologists, who interpret it and decide, based on this information, where they think the different layers of the ground are spatially located, including the locations and extents of the faults. The interpreted data can then be used as the basis for the description of the geo-structure

- Image logs (fracture identification for stress trajectory determination)

- Mini fracture test or Leak test (breakdown pressure and closure stress) to obtain the magnitude of horizontal stresses

- Formation pressure measurements

- Rock core tests (geomechanical properties and rock strength, temperature relative permeability besides the routine core tests) for reservoir rock as well as reservoir upper and lower hanging wall.

Data from these sources are integrated with coupled reservoir-geomechanics modeling to estimate the induced stress and changes in reservoir and surrounding rock properties due to production and injection. These changes may cause shear failure as well as tensile failure in the model changing the reservoir permeability and porosity that should be taken into consideration for safe reservoir-geomechanics calculations and ensuring optimal oil production. The complete workflow for integrating the data from various sources is briefly described below.

Step 1: after acquiring the relevant data, the reservoir “static” model is built in the reservoir simulation software, ECLIPSE, (Fig. 1) which describes all its geological, lithological, stratigraphical and petrophysical aspects. A static reservoir study typically involves four main stages, carried out by experts in the various disciplines:

• Structural modelling: Reconstructing the geometrical and structural properties of the reservoir, by defining a map of its structural top and the set of faults running through it. This stage of the work is carried out by integrating interpretations of geophysical surveys with available well data.

• Stratigraphic modelling: Defining a stratigraphic scheme using well data, which form the basis for well-to-well correlations. The data used in this case typically consist of electrical, acoustic and radioactive logs recorded in the wells, and available cores, integrated where possible with information from specialist studies and production data.

• Lithological modelling: Definition of a certain number

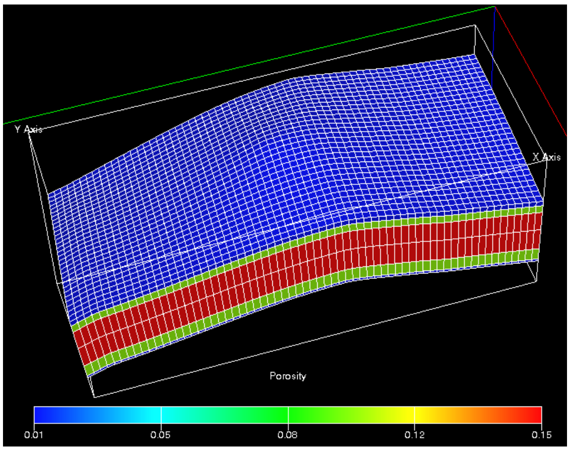

Fig. 1 3D static model: reservoir layering and related porosity

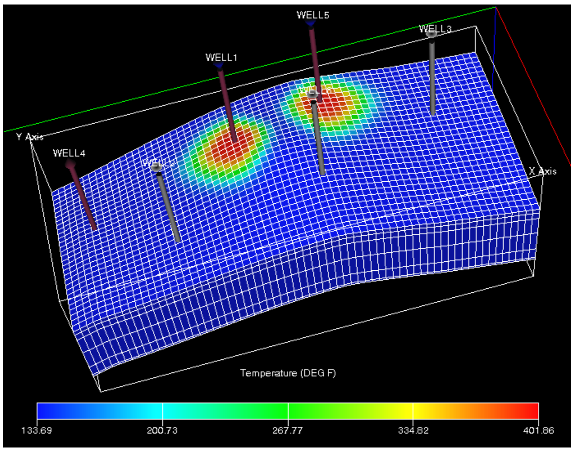

Fig. 2 3D dynamic model: reservoir temperature and wells system

of lithological types (basic facies) for the reservoir in question, which are characterized on the basis of lithology proper, sedimentology and petrophysics. This classification into facies is a convenient way of representing the geological characteristics of a reservoir, especially for the purposes of subsequent three-dimensional modelling.

• Petrophysical modelling: Quantitative interpretation of well logs to determine some of the main petrophysical characteristics of the reservoir rock, such as porosity, water saturation, and permeability. Core data represent the essential basis for the calibration of interpretative processes.

Step 2: The “dynamic” model is built in ECLIPSE which takes as input all the information of the static model and, by introducing a series of additional parameters regarding the characteristics of the fluids, the rock and the well system, provides the information required for the field management, such as the dynamic reserve evaluation injection and the production profiles as a function of the development scenarios (Fig. 2).

Step 3: A three-dimensional geomechanical model is constructed in the mechanical simulation software, ABAQUS, using the property model developed in the previous steps. The geomechanical calculation requires modeling not only of the reservoir but also of its containment (over-, under- and side-burden), to apply

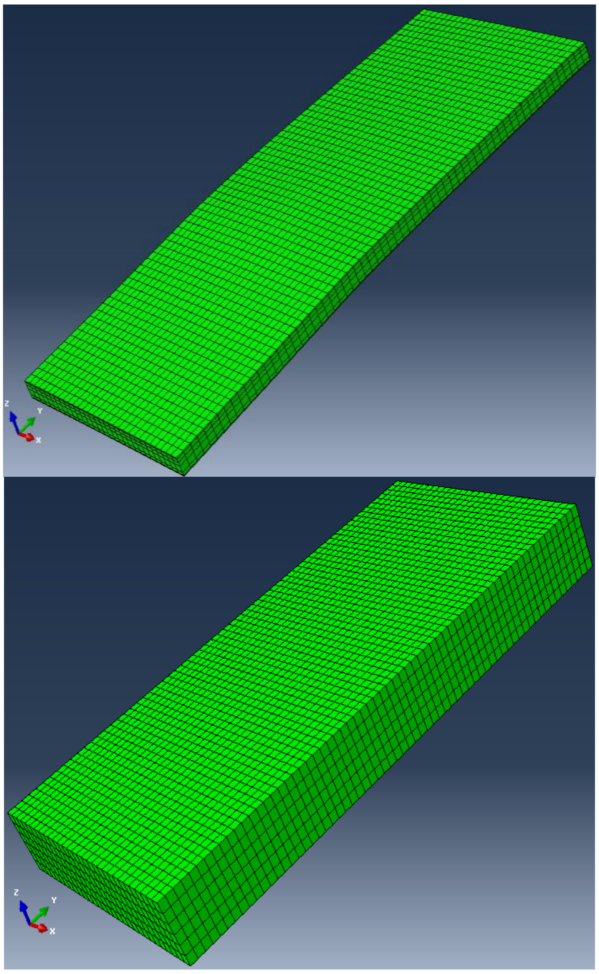

Fig. 3 3D geomechanical model: reservoir (left), and reservoir and its surrounding (right)

boundary conditions and to define the thermo-hydromechanical properties of the reservoir and surrounding rocks (Fig. 3).

So, this 3-D model consists of reservoir, overburden, under-burden and side-burden up to sufficient distance to eliminate any boundary effects that may have on the results. Initial stress analysis is performed to model the far-field state of in-situ stress (pre-injection and pre-production state). The external part (side-burden, over-burden and under-burden) of the grid, needed to correctly simulate the geomechanical behavior of the system, is automatically built by a MATLAB interface code provided that the final model size is given.

It is evident that solving the equations in this great environment, knowing that the majority of the models fall outside the reservoir, will impose enormous computational costs. As a result, it can be separated to two sets of equations that are used for inside and outside of the reservoir. Then, in the reservoir part the flow and equilibrium equations are solved completely assigning 8-node brick stress/displacement/pore pressure/temperature (C3D8PT) and in the outside of the reservoir only equilibrium equations are solved assigning 8-node brick stress/displacement (C3D8).

The initial geostatic stress field must be in equilibrium with the applied loads and boundary conditions. Ideally, the loads and initial stresses should exactly equilibrate and produce zero deformations. This state is obtained performing an initial ABAQUS analysis fixing all displacement degree of freedoms. The calculated reaction forces from the ABAQUS output file are then used to create nodal point forces, which are applied in the first step of the actual ABAQUS analysis.

Step 4: Coupled reservoir-geomechanics modeling is conducted to quantify the changes in in-situ stresses caused due to production or injection. For each scenario, changes in temperature (ΔT) and changes in pressure (ΔP) are computed using the reservoir simulation software, ECLIPSE. Corresponding changes in stresses ($\Delta\sigma$) and volumetric strains ($\Delta\varepsilon$) are computed using ABAQUS.

Step 5: Once the coupled reservoir-geomechanical modeling is constructed for the proposed production and injection plan, the new stress state is obtained and checked against the failure criteria for tensile, shear and other complex failure modes. The stress path and strains calculated from the coupled simulations are used to predict the possible occurrence and location of mechanical failures in the model (both reservoir and containments).

Step 6: Computing the new P and T as below:

The reservoir pore pressure and temperature can be directly used in the geomechanics model (using mapping code). However, the volumetric strain in reservoir model cannot be directly used and different formulations of porosity and permeability are employed for this purpose. Experimental studies performed by Manguy and Longuemare (2002) and Touhidi-Baghini (1998) showed that changes in permeability and porosity are directly related to volumetric strains which are mainly caused by shear failure.

To account for changes in porosity and permeability due to volumetric strains developed in the rock by temperature and pressure, the following equations can be used

$$\phi = \phi_0 + \alpha(\varepsilon_v - \varepsilon_{v0}) + \frac{1}{\varphi}(P - P_0) \qquad (3)$$

$$\ln\frac{k_1}{k_0} = \frac{c}{\phi_0}\varepsilon_v \qquad (4)$$

Where ϕ is porosity, ϕ_0 is initial porosity, k_1 is permeability, k_0 is initial permeability, P is pore pressure and ε_v is volumetric strain. Also, α and φ represent constant parameters (Biot 1940). The values for α and φ for the studied reservoir are one and infinite, respectively. Also, P_0 is the initial reservoir pore pressure and ε_{v0} represents the initial volumetric strain. An appropriate value for c has to be selected. Values for c are derived from the Chardabellas equation. According to Touhidi- Baghini, the values c = 5 and c = 2 appear to be appropriate to match with vertical and horizontal permeability evolutions, respectively (Touhidi-Baghini 1998).

Step 7: mapping the data from reservoir grid to geomechanics grid and vice versa:

Coupling between a geomechanics grid and a reservoir grid is an important issue when the grids coincide but are used to refer to the same spatial domain in a simulation

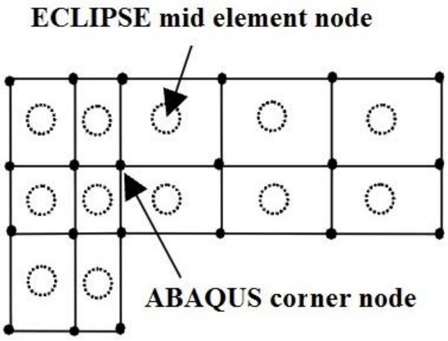

Fig. 4 Adjustment of finite difference and finite element mesh

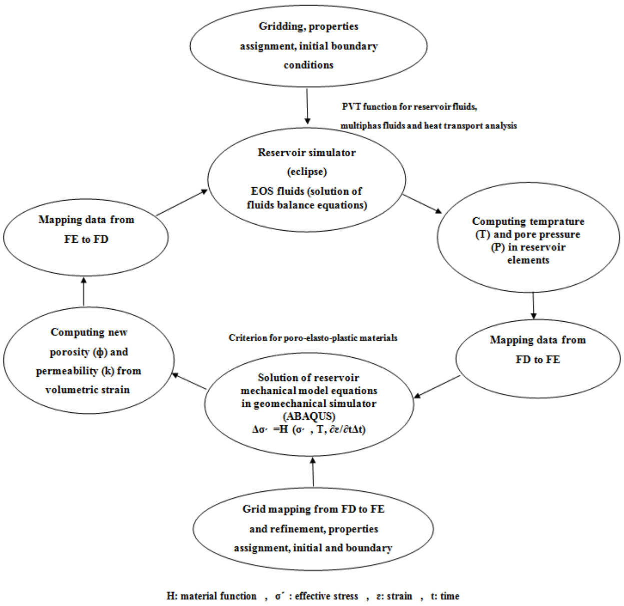

Fig. 5 THM loop (linking between ECLIPSE and ABAQUS)

(Tran *et al.* 2008). The result of coupled solution will depend upon the mapping of information between the two grids.

The fact that the grid type in the reservoir simulator is different from geomechanical simulator makes the mapping process more complicated. In fact, in the reservoir simulator a finite difference grid discretization is used where flow variables are computed at the center of gridblocks while in the geomechanical simulator a finite element grid discretization is used to compute displacements at the nodes of the grid (Fig. 4).

Generally, the reservoir grid in geomechanical simulator is not identical with the reservoir grid in the reservoir simulator. In the reservoir geomechanics simulator, the size of the grid cells is less than reservoir fluid flow simulator, i.e., the reservoir grid in reservoir simulator is coarser than the geomechanics grid which is necessary for accurate stress and strain determination.

Also, in this research, the grids in the reservoir and geomechanical simulators are not coincident, passing the data (temperature, pressure, volumetric strain) between the two simulators is more complex. Therefore, a field transfer algorithm must be used to perform the passing of data from

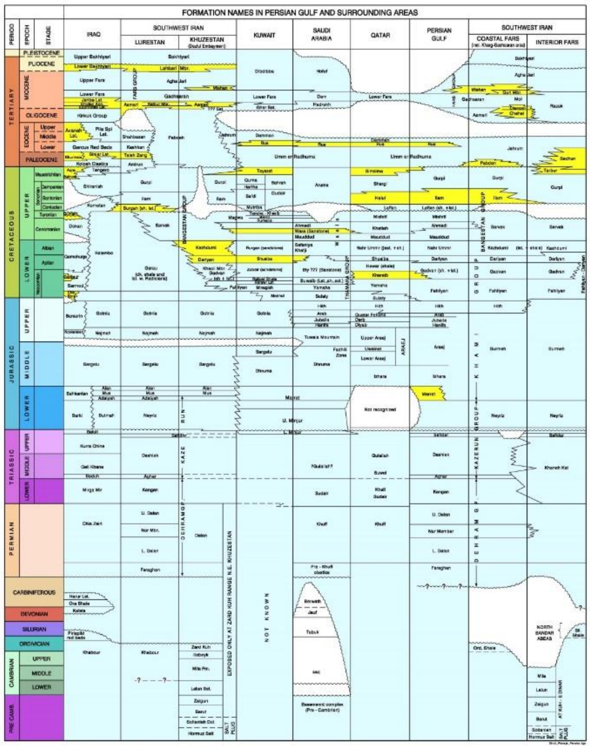

Fig. 6 Generalized Stratigraphic Column of SW IRAN and adjacent area (Setudehnia 1978)

one grid to the other. Here, a development of MATLAB code is used for mapping the data from reservoir grid centers to geomechanics grid nodes and vice versa.

The lateral boundaries of the reservoir are considered with neither thermal nor fluid flow. The constraints for the geomechanical model are as follows. The right, left, front and back sides of the model are fixed in the x-direction and y-direction so there would be no displacement in the x and y directions. The bottom side of the model is fixed in all directions and the top of the model is free to move in all directions.

Fluid flow, thermal and geomechanical coupling modules (step 1 to 7) are shown in Fig. 5.

5. Regional geological setting

The oil regions situated in Khuzestan province were studied as the most oil-rich region in Iran, with the Dezful Embayment in southwest Khuzestan being especially prolific. Most of the oil fields in the region are located in the foothill zone (Zagros Folded zone) of the NW-SE trending Zagros Mountain range having similar trends to the Zagros Mountain range elongated anticline structure, which is called the Zagrous Trends.

The result of drilling in this field and neighborhood fields show that thirteen formations from three groups overlaying one another. The youngest group Fars Group consists of Aghajari and Gachsaran formations, Asmari, Pabdeh, and Gourpi formations, the middle group (Bangestan Group) consists of Ilam, Lafan, Sarvak, and Kazhdumi formations and the oldest group (Khami Group)

Table 1 Mechanical properties of the reservoir layers.

Layer	Thickness (m)	Porosity(%)	Permeability(md)
1	10	1	1
2	25	10	45
3	30	15	45
4	45	15	55
5	25	10	40
6	5	1	2

consists of Darian, Gadvan and Fahliyan formations (Fig. 6).

The Sarvak limestone containing heavy oil is the main productive formation. The thickness and the layer slope of Sarvak formation are approximately constant. The reservoir is approximately 2500 m deep and 140 meters thick. Limestone is the dominant rock type in this reservoir. The reservoir geometry has been indicated by 3-D seismic measurements and six wells drilled in the structure. The mechanical properties and the initial stress profile are required to be incorporated in the geomechanical model and coupled with the flow model in order to be able to study the mutual effect of pressure, temperature and stresses and the resulting effect on integrity and injectivity. The reservoir rock mechanical parameters including, uniaxial compressive strength, Young's modulus and Poisson's ratio were obtained from Dipole sonic imager (DSI) logs, laboratory tests and empirical relationships.

The reservoir Young's modulus, Poisson's ratio, cohesion, friction angle is 20 GPa, 0.22, 3 MPa and 30 degrees, respectively. Also, the reservoir initial pressure is about 22 MPa and densities of water, oil and gas are 1190, 850 and 0.90 Kg/m^3, respectively. Other characteristics of the reservoir layers are given in Table 1.

6. Results and discussion

The reservoir dynamic model is built using the ECLIPSE reservoir simulator, which is a fully implicit, three-phase and 3D finite difference code. The dynamic model takes as input all the information of the static model and by introducing a series of additional parameters regarding the characteristics of the fluids, the rock and the wells system provides the information required for the field management such as the dynamic reserve evaluation and the production and injection profiles as a function of the development scenarios. The dynamic model provides as output sets of data that are used in the geomechanical finite element simulation such as the grid discretization of the reservoir and of the surrounding areas, the initial values of porosity and permeability, the evolution of the fluid pressure and temperature as a function of space and time. As explained in detail in the above section, all the information is converted using an interface code to build the ABAQUS finite element model.

The initial reservoir temperature is 135 degree Fahrenheit (Fº) and the reservoir was targeted using six wells. Production conditions and restrictions are as follows:

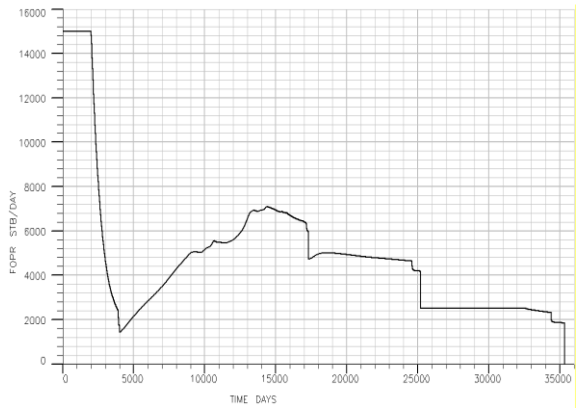

Fig. 7 Reservoir oil production rate

Table 2 reservoir rock thermal properties (Eppelbaum *et al.* 2014)

Heat Capacity (J.cm^{-3}.°C^{-1})	Thermal Conductivity (W. m^{-1}.°C^{-1})	Thermal Expansion Coefficient (°C^{-1})
2.30	2.37	2×10^{-5}

- Each well production minimum bottom hole pressure is 1300 Psi
- Oil production rate of each well is 2,500 stb/day (stock tank barrel per day)
- Oil production of each well terminated if the well production rate is less than300 stb/day or water cut is more than 0.7.

Oil production of all wells started at January first 2007. When production from the first two wells terminated (due to the above- mentioned restrictions) the two wells will be used as steam flooding wells. Injection strategy involves the injection of 10000 stb/day by each well with an injection temperature of 400 Fº and a maximum bottom hole pressure of 4000 Psi.

The reservoir oil production rate is shown in Fig. 7. As shown in the Figure, at the beginning, each well production rate is 2,500 stb/day. As time passes, the oil production rate decreases gradually due to reservoir pressure reduction. After about 4000 days from the start of production, the production rates of wells No.1 and No.5 fall under the predefined limit, so their production will be terminated and these two wells will be prepared for steam injection. After steam injection, the reservoir pressure gradually increased and so the rate of production in four other production wells will increase. By continuing steam flooding from wells No. 1 and No. 5 and oil production for others, oil production of wells will be halted at various times due to the predefined economical restriction.

The in-situ stress regime for the case study is normal faulting stress regime with stress ratio (k) of 0.75 and Mohr-Coulomb elasto-plastic criterion was used for geomechanical simulation of the reservoir. Also, for studding the surrounding rocks the elastic model was used. The surrounding rocks Young's Modulus and Poisson ratio is 30 GPa and 0.20, respectively. The reservoir rock thermal properties are listed in Table 2.

As mentioned above, due to the higher values of injection temperature as compared with the reservoir

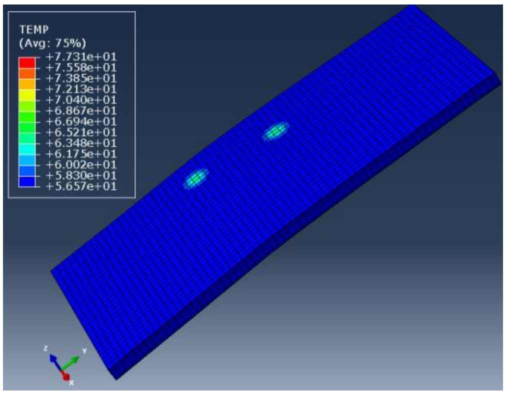

t≈3150 days after injection

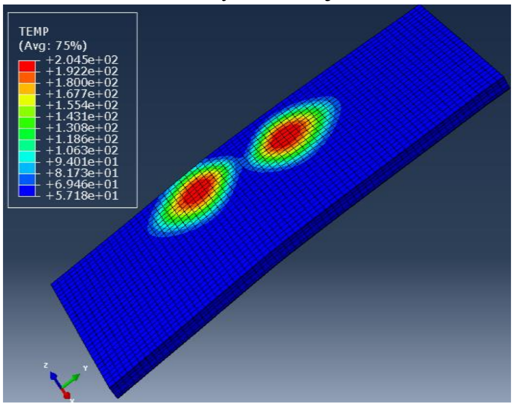

t≈310000 days after injection

Fig. 8 Evolution of temperature in the reservoir

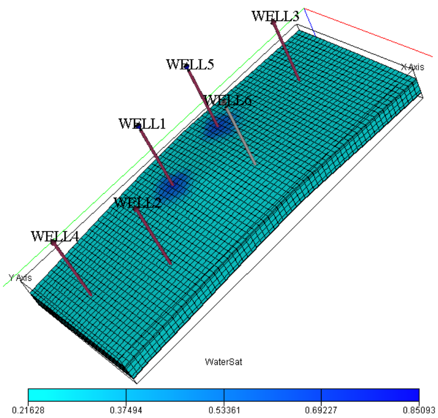

t≈3150 days after injection

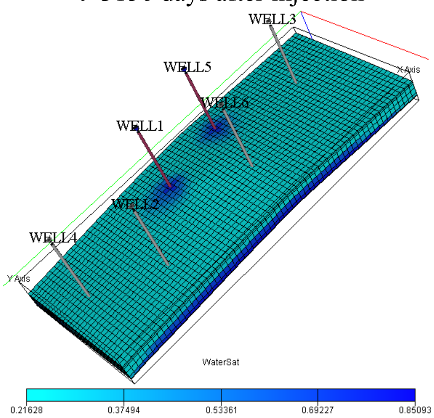

t≈310000 days after injection

Fig. 9 Evolution of water saturation in the reservoir

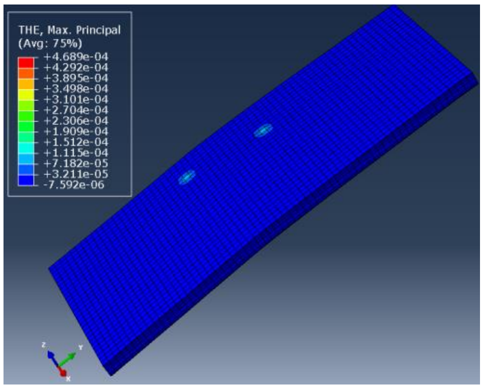

t≈3150 days after injection

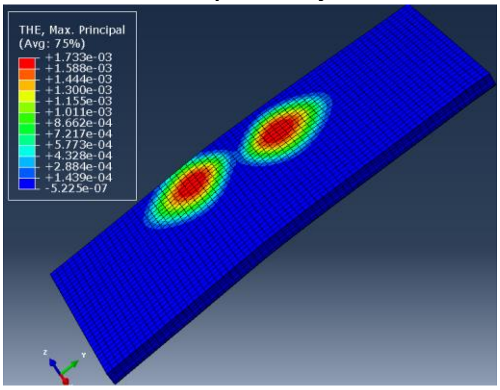

t≈310000 days after injection

Fig. 10 Thermal strain in the reservoir

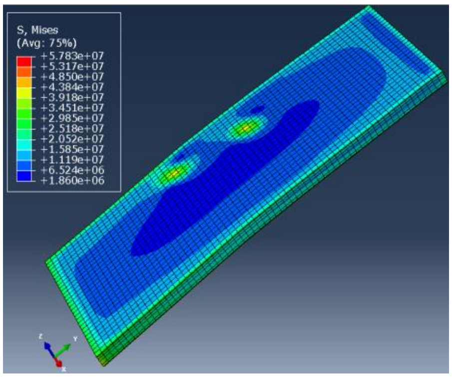

t≈3150 days after injection

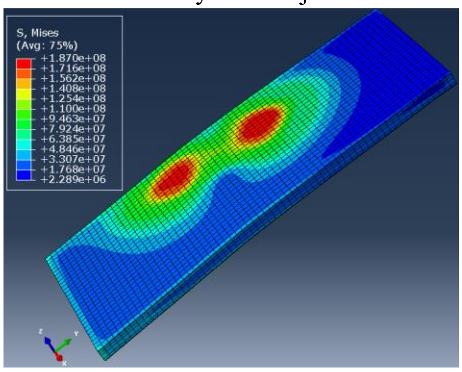

t≈310000 days after injection

Fig. 11 Mises stress distribution

temperature, with increasing injection time, temperature around the injection rises gradually and thermal strain

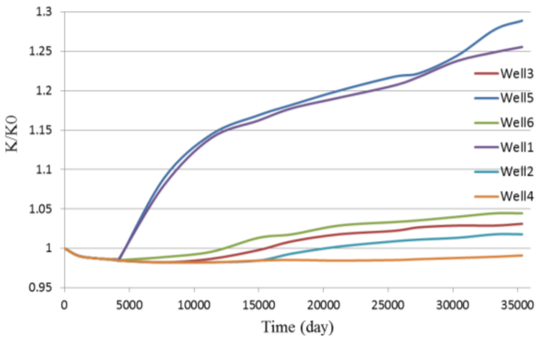

Fig. 12 Reservoir layer 3 permeability variations around the wells

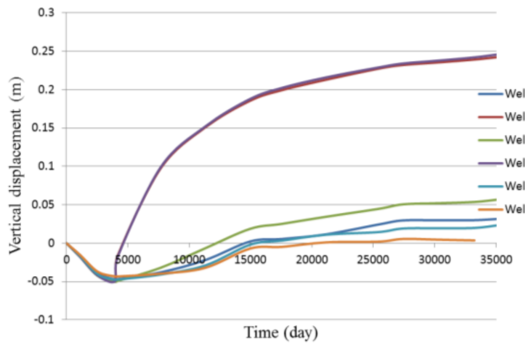

Fig. 14 Vertical displacement changes around Wells

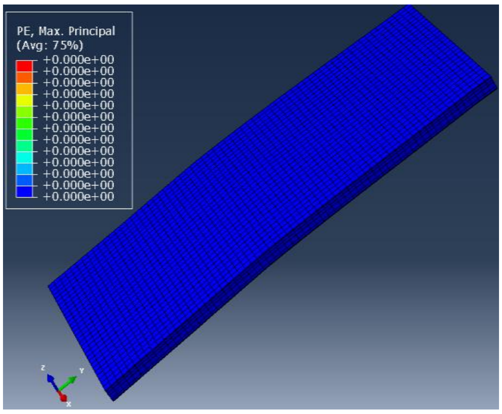

Before injection

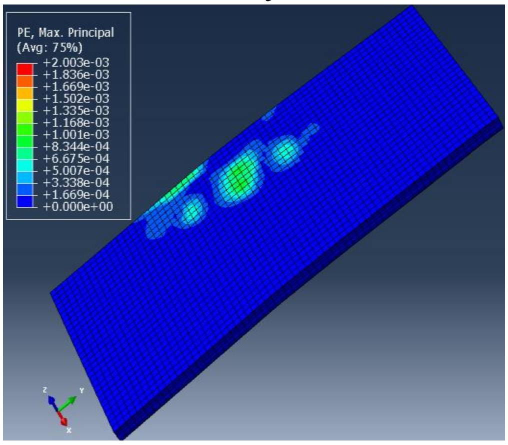

t≈310000 days after injection

Fig. 13 Maximum plastic strain in the reservoir

occurs around injection zone. Fig. 8 shows that the temperature first increases above the injection well and then extends laterally to become uniform in the upper part of the reservoir. This uniformity is related to lateral boundary conditions that were imposed on the model.

Evolution of the reservoir water saturation during steam flooding is shown in Fig. 9 which has the same trend as temperature.

Fig. 10 shows that the evolution of the thermal strain is very similar to that of temperature (Fig. 8), i.e., fast at the start of steam injection in a vertical direction above the injection wells and then slower in the periphery as the steam chamber reaches the top of the reservoir.

Steam injection increases the pore pressure, dilates the rock skeleton and the pore fluid pressure modifies the in situ stresses in a complex set of interactions. Distribution of Von Mises stress during the coupling is shown on Fig. 11.

During each coupling period, variations in pore pressure, temperature, strains and stresses were computed. As explained in previous section 4, in this explicit coupling approach, porosity and permeability in grid cells of the reservoir model have been updated at specified times after computation of stress and strain by the geomechanical simulator and modification of the porosity and permeability values according to Eqs. (3) and (4). The updated porosity and permeability were integrated in the simulation of the next period. Permeability variations (k/k_0) around the reservoir wells in layer 3 are shown in Fig. 12. As shown, permeability increases during injection scenario and increasing rate around injection wells are more than others. Porosity also has approximately same trend.

The finite element analysis of the reservoir showed that during production scenario (before injection) no plastic strain is occurred in the reservoir although during injection scenario and because of high thermal strain, plastic strain is occurred around injection wells (Fig. 13).

During depletion, the reservoir has shown subsidence. However, by injection of wells No.1 and No. 5 and production from other four wells, the reservoir displacement reversed (Fig. 14). As can be observed, the uplift is very fast just above the injection wells resulting in plastic deformation.

7. Conclusions

Numerical modeling is a proper tool to calculate and analyze fluid flow induced stress changes and to estimate their impact on rock stability and important aspect in reservoir management. In addition to the necessity for failure study in reservoirs, the coupling between reservoir simulation and geomechanics is important because flow and temperature differences alter the stresses and reservoir porosity and permeability changing the fluid flow pattern. Therefore, this should be studied in a coupling procedure.

In this paper, the two software ECLIPSE and ABAQUS were linked for analysis of coupled THM processes in complex geological media. The codes were linked with modules representing the coupled thermo-mechanical and hydrologic-mechanical behavior of rocks. The fluid flow simulator was initially executed over a first period (built static and dynamic model). Updated pore pressures at the end of this first period are interpolated and transferred onto the geomechanics grid in the geomechanical simulator using MATLAB code. Based on the updated producing conditions and constitutive relationships, the geomechanical simulator calculates the strains. Then, the reservoir permeability and porosity are modified according to theoretical or empirical functions (between volumetric strain, permeability and porosity). Updated grid block permeabilities and porosities are then transferred to the fluid flow simulator for the execution of the next time period. It was demonstrated that the usefulness of linked, explicit coupled THM analyses for complex problems was associated with steams flooding in an Iranian reservoir. The following conclusions can be drawn for the given parameters and production and injection scenarios through the analysis of the time history study of petrophysical parameters, effective stress and strain:

- Temperature initially increases above the injection well and then extends laterally to become uniform in the upper part of the reservoir.

- Unlike the production scenario (before injection), permeability increases during injection scenario and increasing rate around injection wells exceed those of others. Porosity also follows approximately the same trend.

- During depletion, the reservoir has shown subsidence. However, through injection, displacement reversed.

- The reservoir uplift is very fast just above the injection wells resulting in plastic deformation.

References

Angus, D.A., Dutko, M., Kristiansen, T.G., Fisher, Q.J., Kendall, J.M., Baird, A.F., Verdon, J.P., Barkved, O.I., Yu, J. and Zhao, S. (2015), "Integrated hydro-mechanical and seismic modelling of the valhall reservoir: A case study of predicting subsidence, AVOA and microseismicity", *Geomech. Energy Environ.*, **2**, 32-44.

Biot, M.A. (1940), "General theory of three-dimensional consolidation", *J. Appl. Phys.*, **12**, 155-164.

Closmann, P.J. and Bradley, W.B. (1979), "The effect of temperature on tensile and compressive strengths and young's modulus of oil shale", *SPE J.*, **19**(5), 301-312.

Dusseault, M.B. and Collins, P.M. (2008), *Geomechanics Effects in Thermal Processes for Heavy Oil Exploitation*, CSEG Recorder, 20-23.

Elyasi, A., Goshtasbi, K. and Hashemolhosseini, H. (2016), "A coupled geomechanical reservoir simulation analysis of CO_2-EOR: A case study", *Geomech. Eng.*, **10**(4), 423-436.

Elyasi, A., Goshtasbi, K. and Hashemolhosseini, H. (2016), "Coupled solid and fluid mechanics simulation for estimating optimum injection pressure during reservoir CO2-EOR", *Struct. Eng. Mech.*, **59**(1), 37-57.

Eppelbaum, L., Kutasov, I. and Pilchin, A. (2014), "Thermal properties of rocks and density of fluids", *Appl. Geotherm.*, 99-149.

Goodarzi, S., Settari, A., Zoback, M. and Keith, D. (2010), "Thermal aspects of geomechanics and induced fracturing in CO_2 injection with application to CO_2 sequestration in Ohio River Valley", *Proceedings of the Society of Petroleum Engineers International Conference on CO_2 Capture*, Storage, and Utilization, Louisiana, U.S.A., November.

Handing, J. and Hager. R.V.J. (1957), "Experimental deformation of sedimentary rocks under confining pressure: Tests at room temperature on dry samples", *Bullet. Am. Assoc. Petrol. Geolog.*, **41**(1), 1-50.

Horsrud, P., SØnstebØ, E.F. and BØe, R. (1998), "Mechanical and petrophysical properties of North Sea shales", *Int. J. Rock Mech. Min. Sci.*, **35**(8), 1009-1020.

Kolditz, O., Gorke, U.J., Shao, H. and Wang, W. (2012), *Thermo-Hydro-Mechanical-Chemical Processes in Porous Media: Benchmarks and Examples*, Heidelberg, Springer.

Lamy-Chappuis, B., Angus, D.A., Fisher, Q., Grattoni, C.A. and Yardley, B.W.D. (2014), "Rapid porosity and permeability changes of calcareous sandstone due to CO_2-enriched brine injection", *Geophys. Res. Lett.*, **41**(2), 399-406.

Lempp, C. and Welte, D.H. (1994), "The effect of temperature on rock mechanical properties and fracture mechanisms in source rocks experimental results", *Proceedings of the Rock Mechanics in Petroleum Engineering*, Delft, the Netherlands, August.

Longuemare, P., Mainguy, M., Lemonnier, P., Onaisi, A., Gerard, C. and Koutsabeloulis, N. (2002), "Geomechanics in reservoir simulation: Overview of coupling methods and field case study", *Oil Gas Sci. Technol.*, **57**(5), 471-483.

Lynch, T., Fisher, Q., Angus. D.A. and Lorinczi, P. (2013), "Investigating stress path hysteresis in a CO_2 injection scenario using coupled geomechanical-fluid flow modelling", *Energy Proc.*, **37**, 3833-3841.

Mainguy, M. and Longuemare, P. (2002), "Coupling fluid flow and rock mechanics: Formulations of the partial coupling between reservoir and geomechanical simulators", *Oil Gas Sci. Technol.-Rev. IFP*, **57**(4), 355-367.

Setudehnia, A. (1978), "The mesozoic sequence in southwest Iran and adjacent area", *J. Petrol. Geol.*, **1**(1), 3-42.

Touhidi-Baghini, A. (1998), "Absolute permeability of McMurray formation oil sands at low confining stresses", Ph.D. Dissertation, University of Alberta, Alberta, Canada.

Tran, D., Buchanan, L. and Nghiem, L. (2008), "Improved gridding technique for coupling geomechanics to reservoir flow", *Proceedings of the Annual Technical Conference and Exhibition*, Denver, Colorado, U.S.A., September.

Wang, W., Kosakowski, G. and Kolditz, O. (2009), "A parallel finite element scheme for thermo-hydro-mechanical (THM) coupled problems in porous media", *Comput. Geosci.*, **35**(8), 1631-1641.

Watanabe, N., Wang, W., McDermott, C., Taniguchi, T. and Kolditz, O. (2010), "Uncertainty analysis of thermo-hydro-mechanical coupled processes in heterogeneous porous media", *Comput. Mech.*, **45**(4), 263-280.

CC